Evaluation of Dose Calculation Based on Cone-Beam CT Using Different Measuring Correction Methods for Head and Neck Cancer Patients

Hanshun Gong, MS[1],[*] (ID), **Bo Liu, PhD**[2],[*], **Gaolong Zhang, PhD**[3], **Xiangkun Dai, MS**[1], **Baolin Qu, MD**[1], **Boning Cai, MD**[1], **Chuanbin Xie, MS**[1], **and Shouping Xu, PhD**[4],[5] (ID)

Abstract

Purpose: To investigate and compare 2 cone-beam computed tomography (CBCT) correction methods for CBCT-based dose calculation. **Materials and Methods:** Routine CBCT image sets of 12 head and neck cancer patients who received volumetric modulated arc therapy (VMAT) treatment were retrospectively analyzed. The CBCT images obtained using an on-board imager (OBI) at the first treatment fraction were firstly deformable registered and padded with the kVCT images to provide enough anatomical information about the tissues for dose calculation. Then, 2 CBCT correction methods were developed and applied to correct CBCT Hounsfield unit (HU) values. One method (HD method) is based on protocol-specific CBCT HU to physical density (HD) curve, and the other method (HM method) is based on histogram matching (HM) of HU value. The corrected CBCT images ($CBCT_{HD}$ and $CBCT_{HM}$ for HD and HM methods) were imported into the original planning system for dose calculation based on the HD curve of kVCT (the planning CT). The dose computation result was analyzed and discussed to compare these 2 CBCT-correction methods. **Results:** Dosimetric parameters, such as the D_{mean}, D_{max} and $D_{5\%}$ of the target volume in CBCT plan doses, were higher than those in the kVCT plan doses; however, the deviations were less than 2%. The $D_{2\%}$, in parallel organs such as the parotid glands, the deviations from the $CBCT_{HM}$ plan dose were less than those of the $CBCT_{HD}$ plan dose. The differences were statistically significant ($P < .05$). Meanwhile, the V_{30} value based on the HM method was better than that based on the HD method in the oral cavity region ($P = .016$). In addition, we also compared the γ passing rates of kVCT plan doses with the 2 CBCT plan doses, and negligible differences were found. **Conclusion:** The HM method was more suitable for head and neck cancer patients than the HD one. Furthermore, with the $CBCT_{HM}$-based method, the dose calculation result better matches the kVCT-based dose calculation.

Keywords

adaptive radiation therapy, cone-beam computed tomography, deformable image registration, Hounsfield unit (HU), HU-density map, histogram matching algorithm

[1] Department of Radiation Oncology, The First Medical Center of PLA General Hospital, Beijing, China

[2] School of Astronautics, Beihang University, Beijing, China

[3] School of Physics, Beihang University, Beijing, China

[4] Department of Radiation Oncology, National Cancer Center/Cancer Hospital, Chinese Academy of Medical Sciences and Peking Union Medical College, Beijing, China

[5] National Cancer Center/National Clinical Research Center for Cancer/Hebei Cancer Hospital, Chinese Academy of Medical Sciences, Langfang, China

*Hanshun Gong and Bo Liu contribute equally to this work.

Corresponding Author:

Shouping Xu, Department of Radiation Oncology, National Cancer Center/Cancer Hospital, Chinese Academy of Medical Sciences and Peking Union Medical College, Beijing, China.

Email: shouping_xu@yahoo.com

Abbreviations:
HU, Hounsfield unit; CBCT, cone-beam computed tomography; kVCT, kilovoltage computed tomography; OBI, on-board imager; RT, radiation therapy; ART, adaptive radiation therapy; HD, HU-value to the physical density; HM, histogram matching; OARs, organs at risk; pGTVnx, gross tumor volume; pGTVnd, positive lymph nodes; SDH, standard dose head; HQH, high quality head; LDT, low dose thorax; PTV, planning target volume; GUI, graphical user interface; RR, rigid registration; DIR, deformable image registration; SGD, stochastic gradient descent; CERR, Computational Environment for Radiotherapy Research; L-E-T, larynx esophagus trachea; DVHs, dose-volume histograms.

Introduction

Cone-beam computed tomography (CBCT) has been widely used for patient positioning in radiation therapy (RT), and CBCT-based dose calculation has attracted increasing attention.[1,2] CBCT images comprise essential anatomical information about patients, embodying changes in anatomical structures during treatment; these changes lay a vital foundation for individual adaptive radiation therapy (ART).[3,4] Setup errors, respiratory movement, organ movements, and shrinkage will cause dose differences during RT delivery.[5] Therefore, in precise RT, it is essential to evaluate the factors that may cause the dose variation in the treatment process and adequately determine whether re-planning is necessary.[6] Through the rigid or deformable image registration between CBCT and kilovoltage computed tomography (kVCT), the dosimetric changes due to the patient weight loss can be evaluated to determine the re-planning necessity.[7-9]

The kVCT and CBCT modalities differ significantly in several aspects, such as the equipment's physical structure, the image acquisition parameters, and the image reconstruction techniques, resulting in discrepancies in image quality and Hounsfield unit (HU) values. The quality of CBCT images is more susceptible to the size of scanning sites, the target volume's (TV's) density, and the adjacent tissues around the tumor.[10,11] Related topics have been widely considered in recent years, including whether the CBCT-based dose calculation accuracy can meet the clinical demand and how to improve the accuracy for actual patients. Scholars have tried various correction methods,[12-15] including deformable registration methods,[16,17] machine learning and deep learning methods.[18-20] Richter et al[21] found that the HU value of CBCT images (Elekta XVI system) directly correlated with the scanning conditions. For different tumor sites, appropriate correction strategies should be considered regarding the accuracy of CBCT-based dose calculations. The dose differences between CBCT- and kVCT-based calculation have been reported to be $14.5\% \pm 10.4\%$ for the standard CT curve, $1.4\% \pm 2.4\%$ for the phantom, $1.3\% \pm 2.3\%$ for all patients, and $1.5\% \pm 2.5\%$ for head patients. Dunlop et al[22] evaluated the accuracy of 2 dose calculation methods (physical scattering correction and density coverage methods) in CBCT for head and neck sites. They also evaluated and verified the accuracy of the results obtained by the density distribution method for the CBCT plans using the RayStation treatment planning system (TPS). The average dose difference caused by all CT calibration methods was less than 1%, and the scattering correction method was shown to have the best (0.5%) results. Hu et al[23] studied the dose calculation accuracy for the CBCT images of head and neck cancer patients; they used the HU-value referring to the physical density (HD) curve matching method. The resulting differences were all less than 1%. Zhang et al[24] reduced the difference between intensity-modulated radiation therapy (IMRT) plans for nasopharyngeal carcinoma (NPC) patients with CBCT- and kVCT-based treatment plans to less than 2%. This study was conducted using the approximate correction method of the HD curve for CBCT images of NPC patients. Kurz et al[25] used cycleGAN to correct the CBCT-based treatment plan in dose calculation, which improved the dose calculation accuracy for volumetric modulated arc therapy (VMAT) treatment plans. The passing rates were 100% and 89%, respectively, with 2% and 1% dose difference criteria. The above studies show that methods used to identify a more accurate and rapid method for dose calculation in CBCT images can differ.

This study aimed to evaluate the feasibility of and compare 2 CBCT dose calculation methods for head and neck cancer patients in clinical practice. One corrected the HU value of CBCT based on protocol-specific CBCT HD curve, and the other based on histogram matching (HM). Corrective methods for HU values were investigated based on our previous study,[26] and the guidance and challenges for clinical implementation were discussed.

Materials and Methods

Patient Data

The medical ethics committee of the Chinese PLA General Hospital approved this study (S2016-122-01), and all methods were performed under relevant guidelines and regulations. The requirement for informed consent was waived with the ethics committee's approval, given that patient anonymity was ensured.

Twelve histologically proven locoregionally advanced hypopharyngeal cancer patients treated with Clinac iX (Varian, USA) in our hospital were randomly selected and used to conduct retrospective studies. All patients underwent kVCT scanning with a slice thickness of 3 mm on a Siemens CT system (SOMATOM Definition AS, Germany). During the imaging process, the patients were immobilized with a

thermoplastic head-and-shoulder mask in the supine position and a head-and-shoulder immobilization board. The CT images were transmitted into an Eclipse (Version 10.0) workstation. The enhanced CT, MRI, or PET-CT images were also included and fused to guide the contouring of the TVs and organs at risk (OARs). Each patient received a total of 33 fractions RT. The prescription dose was given 70 Gy to the gross tumor volume (GTV), and positive lymph nodes (pGTVnx and pGTVnd were formed by expanding the corresponding GTV and nodes with a margin of 3-5 mm), and 60 Gy to the high-risk planning target volume (PTV). Finally, VMAT plans with 2 entire arcs were optimized via the RapidArc technique. These plans were delivered for the patient's treatment.

CBCT Image Acquisition

The CBCT images of patient cases were acquired using the on-board imager (OBI) system. The CBCTs were scanned in the half-fan mode for 9 cases with a large FOV to include the shoulder region. The CBCTs of the remaining 3 cases were scanned in full-fan mode. All the images were reconstructed with a 3 mm slice thickness. To exclude the dose calculation deviation caused by the changes in patient anatomical structure during the treatment, we utilized the CBCT images acquired at the first treatment fraction as a correction basis.

CBCT Dose Calculation and Evaluation

In-house ART system software was developed and used in this study. This software contains modules for rigid registration (RR), deformable registration, and dose mapping. The registration module was designed based on a widely used open-source Elastix registration tool.[27] Figure 1 shows the ART system's registration graphical user interface (GUI).

Deformable registration between CBCT and kVCT. The planning CT images, anatomical structure files, planning parameter files, and dose files of the treatment plan, including the CBCT images acquired at the first treatment fraction, were saved in DICOM (Digital Imaging and Communications in Medicine) format. They were imported into the in-house ART system. And then, the CBCT images were rigidly registered to the corresponding kVCT images by matching the bony structures; in this process, only translation and rotation were considered. The RR results were verified by visual checking of an experienced physician. If necessary, further manual adjustments would perform. Afterward, based on the RR result, the CBCT image was further deformably registered to the kVCT image based on the B-spline deformation model. The software applied a multi-resolution registration strategy with the B-spline grid spacing set to 32, 16, and 8 mm. As the scanning range of CBCT was much smaller than kVCT in the superior-inferior direction, a registration region of interest was manually set on the strength of kVCT to decrease the discrepancy. The mutual-information similarity metric was applied for both rigid and deformable registration, and it was optimized using the adaptive stochastic gradient descent optimizer. The registration result was visually examined by fusing the deformed CBCT to kVCT images, and it was adequate for all studied cases. The resulting deformation fields
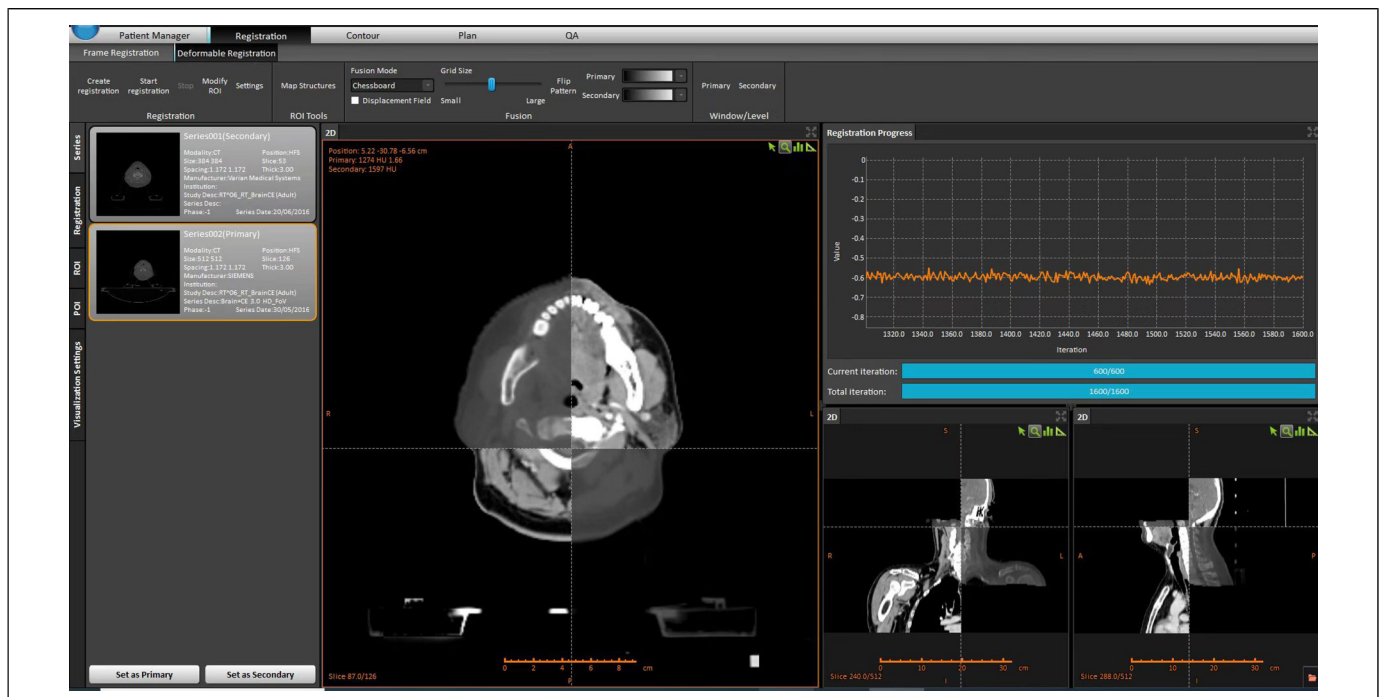

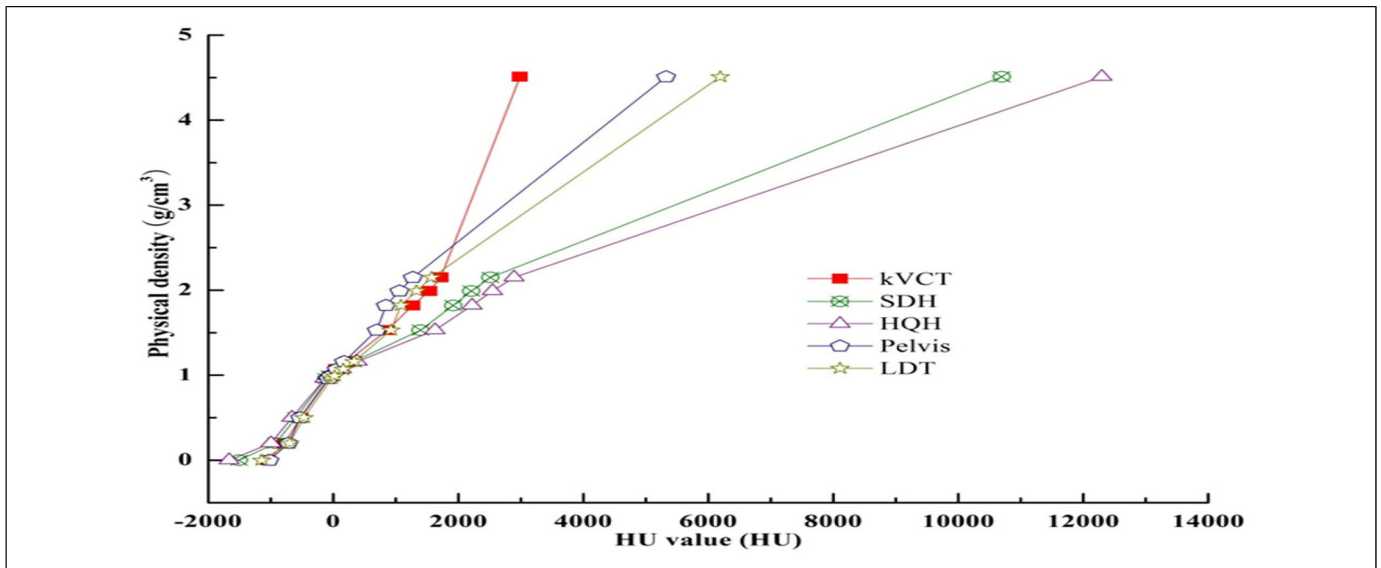**Figure 1.** The registration interface of the in-house ART software.

Figure 2. HU-electron density conversion curves under different scanning conditions. An optional titanium rod core insertion with a physical density of 4.51 accounts for extraordinarily high HU values.
Abbreviations: HU, Hounsfield unit; kVCT, kilovoltage computed tomography; SDH, standard dose head; HQH, high-quality head; LDT, low dose thorax.
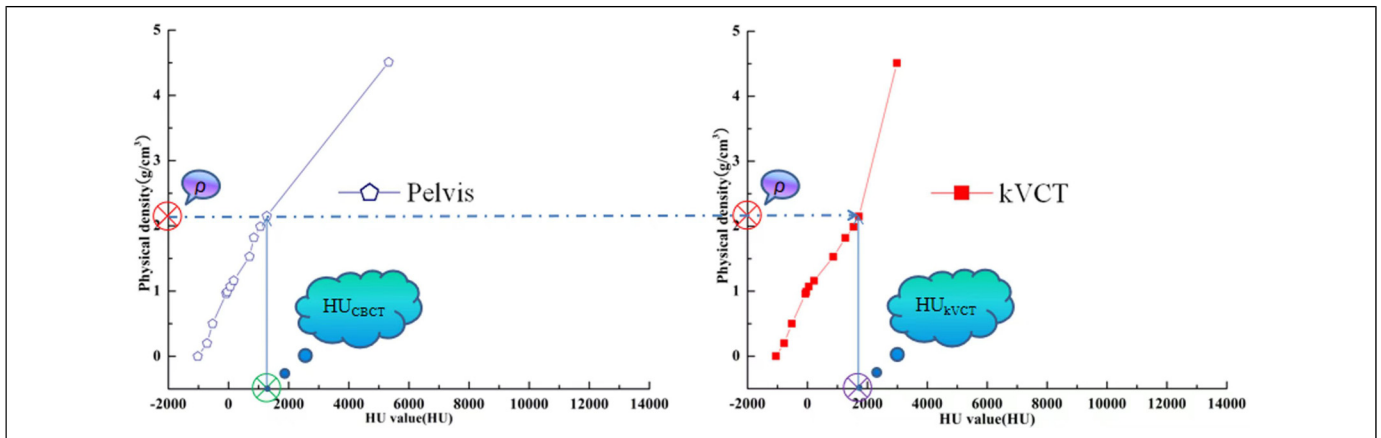

Figure 3. Schematic diagram of conversion between HU values of CBCT(HU_{CBCT}) and its corresponding kVCT(HU_{kVCT}).

were used for deforming the CBCT images into the space of the kVCT image.

CBCT correction based on HU-density curve and HM. Images of the electron density phantom (Model 062M, CIRS, USA) were acquired under standard dose head (SDH), high-quality head (HQH), pelvic and low dose thorax (LDT) settings. RW3 solid water of 5 cm thickness was added to the front and back of the CIRS phantom to avoid unwanted scattering artifacts due to the lack of enough compensation material.[14] The phantom images acquired were transmitted into the TomoCon PACS3 system (TatraMed, Bratislava, Slovak Republic) and saved in DICOM format. With this software tool, the mean and standard deviations of HU values for plug-ins of different materials were obtained, and the HD curves for each clinical scanning condition (SDH, HQH,

pelvis, and LDT) were also created, as shown in Figure 2. Corrected CBCT images were obtained by mapping the HU values of CBCT to physical density using the HD curve of the CBCT and then mapping the resulting density to kVCT HU based on the HD curve of the kVCT as shown in Figure 3. The resulting kVCT images were named $CBCT_{HD}$ in the following.

Another set of corrected CBCT images was generated by HM. Based on the integral histogram of the HU values of kVCT images, CBCT HU values were modified to produce the new CBCT images. After modification, the histograms of the kVCT and CBCT images were matched at 7 quantile values.[28] The resulting corrected images were named $CBCT_{HM}$ in the following.

Dose calculation and comparison. Due to the small size of FOV in the superior-inferior direction, CBCT cannot acquire enough

Table 1. The Percentage Deviation (Mean ± Std) of the CBCT$_{HD}$ and CBCT$_{HM}$ Plan Doses About the kVCT Plan Doses for Different Dosimetric Parameters, Along with the t and P Values of the Paired t-test between the Deviations of CBCT$_{HD}$ and CBCT$_{HM}$ Plan Doses.

		Percentage deviation of the CBCT$_{HD}$ plan doses (%)	Percentage deviation of the CBCT$_{HM}$ plan doses (%)	t	P
pGTV$_{nx}$	D$_{mean}$	0.31 ± 0.45	0.18 ± 0.24	1.01	.334
	D$_{max}$	0.49 ± 0.92	0.31 ± 1.23	0.92	.376
	D$_{5\%}$	0.39 ± 0.43	0.27 ± 0.39	0.84	.418
	D$_{95\%}$	0.31 ± 0.47	0.18 ± 0.21	0.98	.349
	V$_{95\%}$	-0.01 ± 0.02	-0.23 ± 0.46	1.89	.085
	V$_{100\%}$	-0.29 ± 1.32	-0.41 ± 0.85	0.43	.674
pGTV$_{nd}$	D$_{mean}$	0.16 ± 0.55	0.08 ± 0.34	0.82	.431
	D$_{max}$	0.84 ± 1.09	0.43 ± 0.83	2.05	.063
	D$_{5\%}$	0.58 ± 0.86	0.29 ± 0.54	1.79	.099
	D$_{95\%}$	-0.06 ± 0.37	0 ± 0.25	-0.75	.468
	V$_{95\%}$	-0.04 ± 0.07	-0.04 ± 0.06	-0.13	.896
	V$_{100\%}$	-1.52 ± 1.28	-1.15 ± 1.14	-1.15	.272
PTV	D$_{mean}$	0.57 ± 0.44	0.48 ± 0.45	0.54	.601
	D$_{max}$	1.21 ± 1.11	0.80 ± 1.18	1.45	.175
	D$_{5\%}$	0.40 ± 0.52	0.20 ± 0.26	1.54	.152
	D$_{95\%}$	0.24 ± 0.36	0.31 ± 0.39	-0.73	.483
	V$_{95\%}$	-0.07 ± 0.08	-0.06 ± 0.14	-0.20	.844
	V$_{100\%}$	-0.25 ± 0.49	-0.15 ± 0.62	-0.94	.367
Parotid-L	D$_{mean}$	-0.42 ± 0.64	-0.27 ± 0.59	-1.33	.210
	D$_{2\%}$	-0.54 ± 0.28	-0.14 ± 0.49	-3.62	.004
	V$_{10}$	-0.84 ± 0.69	-0.79 ± 0.61	-0.98	.349
	V$_{20}$	-0.58 ± 0.78	-0.64 ± 0.72	0.92	.379
Parotid-R	D$_{mean}$	-0.34 ± 0.75	-0.23 ± 0.74	-1.74	.110
	D$_{2\%}$	-0.38 ± 0.61	0.07 ± 0.79	-2.96	.013
	V$_{10}$	-0.74 ± 0.92	-0.63 ± 1.05	-1.27	.231
	V$_{20}$	-0.74 ± 0.75	-0.93 ± 0.80	1.28	.228
Oral cavity	D$_{mean}$	-0.80 ± 0.50	-0.27 ± 0.68	-2.99	.012
	D$_{2\%}$	-0.67 ± 0.51	-0.04 ± 0.92	-3.23	.008
	V$_{30}$	-1.99 ± 2.04	-0.89 ± 1.75	-2.83	.016
L-E-T	D$_{mean}$	1.40 ± 1.12	0.98 ± 1.13	2.37	.056
	D$_{2\%}$	1.47 ± 1.13	1.16 ± 1.25	2.47	.048
	V$_{30}$	-0.09 ± 0.93	-0.37 ± 0.95	1.76	.130
Cord	D$_{mean}$	-0.24 ± 0.82	-0.12 ± 0.90	-1.03	.325
	D$_{2\%}$	0.05 ± 0.87	0.21 ± 0.59	-1.02	.329

Abbreviations: pGTVnx, gross tumor volume; pGTVnd, positive lymph nodes; PTV, planning target volume; L-E-T, larynx esophagus trachea; kVCT, planning CT; CBCT$_{HD}$, the HD curve of kVCT (planning CT) was used for the transformation process of the CBCT plans; CBCT$_{HM}$, the histogram matching algorithm (HM) was used to correct the HU values of the CBCT plans.

tissue information for dose calculation. To address this issue, the CBCT$_{HD}$ and CBCT$_{HM}$ were padded with the kVCT at the bottom and the top to provide missed anatomy information and thus to fully consider the scattered dose and reduce the dose calculation deviation in CBCT$_{HD}$ and CBCT$_{HM}$.

The generated CBCT$_{HD}$ and CBCT$_{HM}$ images, along with the planning parameter and organ structure files of RT plans, were imported into the Eclipse planning system (Varian, USA). The same dose calculation algorithm was utilized to compute the CBCT$_{HD}$ and CBCT$_{HM}$ plan doses using the HD curve of kVCT images. The 2 CBCT plan doses were compared with those of the original plans in respect of the dosimetric parameters: D$_{mean}$, D$_{max}$, D$_{5\%}$, D$_{95\%}$, V$_{95\%}$, and V$_{100\%}$ for the targets, and D$_{mean}$, D$_{max}$, D$_{2\%}$, and V$_x$ for the OARs.

The images and dose distribution data of kVCT, CBCT$_{HD}$, and CBCT$_{HM}$, were finally imported into the Computational Environment for Radiological Research (CERR) (Version 5.1) (developed by the University of Washington) for analysis. The kVCT dose distribution was employed as the golden standard; the CBCT$_{HD}$ and CBCT$_{HM}$ results were quantitatively evaluated through the γ analysis with criteria of 3%/3 mm and 2%/2 mm with a dose threshold of 5%.

Statistical Analyses

Statistical analyses (paired t-test) were performed in SPSS 17.0 (SPSS Inc., Chicago, IL, USA). Dosimetric parameters and γ analysis were used to evaluate the 2 different dose calculation methods on CBCT-based plans with a P-value <.05.

Results

Analysis of Dose Distribution

The D$_{mean}$, D$_{max}$, and D$_{5\%}$ for the TVs (pGTV$_{nx}$, pGTV$_{nd}$, and PTV) of CBCT$_{HD}$ and CBCT$_{HM}$ plan doses were higher than those of the kVCT doses in all 12 patients. However, the deviations were less than 2%. CBCT$_{HM}$ plan doses were closer to kVCT plan doses than CBCT$_{HD}$ plan doses, but the difference was insignificant. The TV V$_{95\%}$ and V$_{100\%}$ values of CBCT$_{HD}$ and CBCT$_{HM}$ plan doses were less than those of the kVCT plan doses, but there were no significant differences. The deviation of V$_{100\%}$ for pGTV$_{nd}$ was relatively significant compared with other TVs, at -1.52% and -1.15% for CBCT$_{HD}$ and CBCT$_{HM}$ plan doses, respectively.

The D$_{mean}$, V$_{10}$, and V$_{20}$ for the left and right parotid glands (parotid-L and parotid-R) of the CBCT$_{HD}$ and CBCT$_{HM}$ plan doses were smaller than those of kVCT plan doses. There was no significant difference between CBCT$_{HD}$ and CBCT$_{HM}$ plan doses. However, D$_{2\%}$ of CBCT$_{HM}$ plan doses was significantly less than D$_{2\%}$ of CBCT$_{HD}$ and closer to kVCT plan doses ($p = .004$ and .013 for parotid-L and parotid-R, respectively). HM-based CBCT correction provided better results of the plan's D$_{mean}$, D$_{2\%}$, and V$_{30}$ compared with the HD-based calibration for the oral cavity, and the advantage is not negligible. On the other hand, the differences in the D$_{mean}$ and V$_{30}$ values of the larynx-esophagus-trachea (L-E-T) were not statistically significant. However, the D$_{2\%}$ values of the CBCT$_{HM}$ plan dose were closer to those from kVCT images, which was statistically significant ($p = .048$). Compared with other parallel organs, only the parameters of D$_{mean}$ and D$_{2\%}$ were analyzed for the serial organ (the spinal cord). In summary, using the above 2 methods to correct CBCT images for planning provides an insignificant outcome. Details are shown in Table 1. Figures 4 and 5 show the dose-volume histograms (DVHs) and dose distribution of kVCT, CBCT$_{HD}$, and kVCT$_{HM}$ plan doses of a
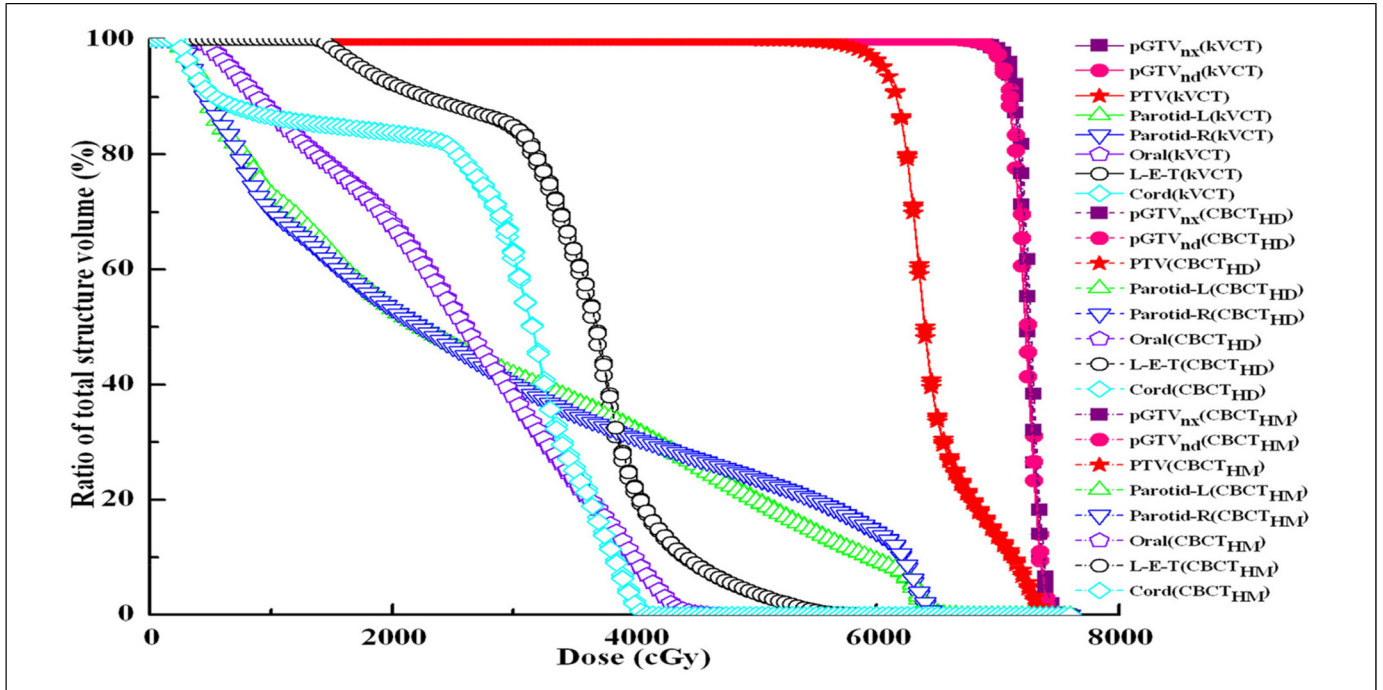
Figure 4. Dose-volume histograms of kVCT, CBCT$_{HD}$, and CBCT$_{HM}$ plan doses for a representative case in half-fan scanning mode.
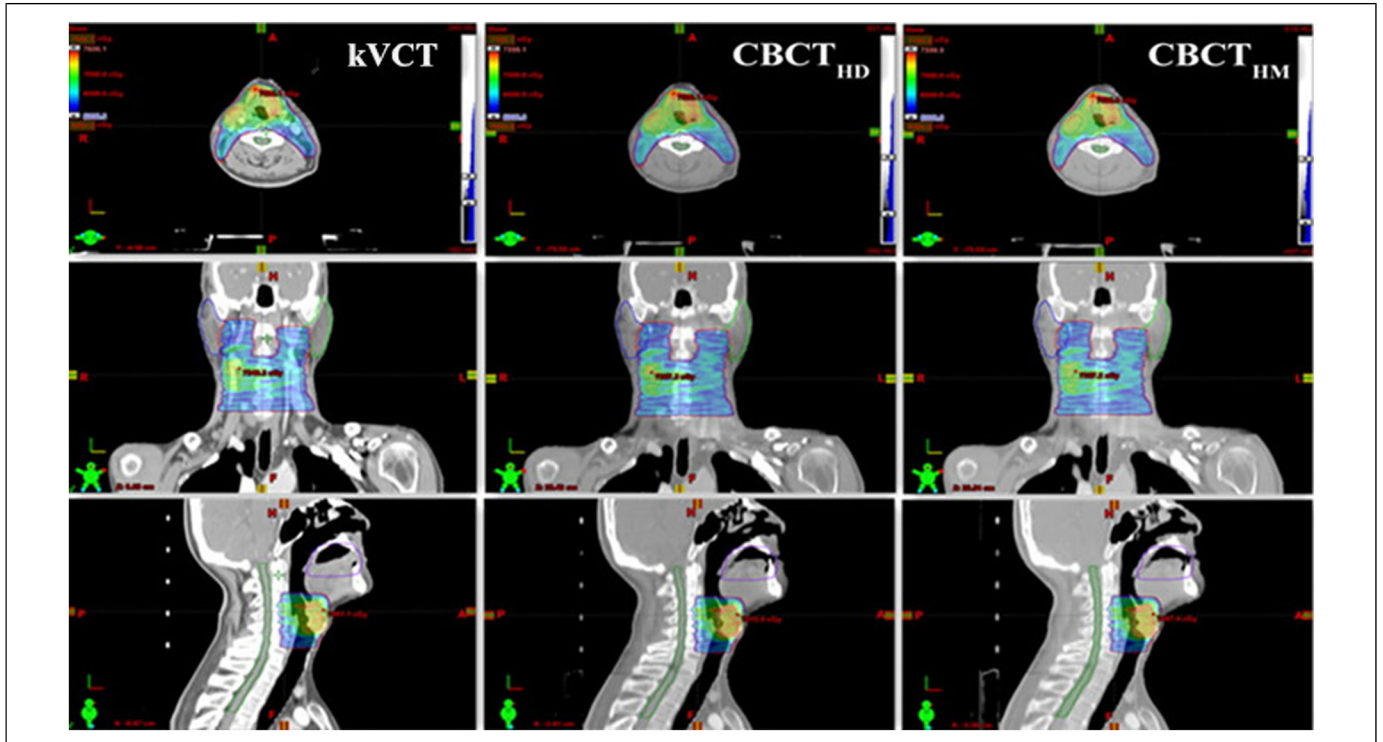

Figure 5. Dose distribution of kVCT (left column), CBCT$_{HD}$ (middle column), and CBCT$_{HM}$ (right column) doses for a representative case in half-fan scanning mode.

typical case in full-fan and half-fan scanning modes, respectively.

Gamma Analysis Results

Tables 2 and 3 show the γ passing rates for all 12 patients at 3%/3 mm and 2%/2 mm criteria, respectively.

For pGTVnx and pGTVnd in all patient plans, regardless of whether the 3%/3 mm or 2%/2 mm criterion was applied, the average γ passing rates of the CBCT plan doses obtained by the HM and HD methods relative to those of kVCT plan doses were both higher than 96%, and there were no significant differences between them. For PTV, the γ passing rates of CBCT$_{HM}$ and CBCT$_{HD}$ plan doses were higher than 98% at 3%/3 mm. The passing rates dropped at the 2%/2 mm criteria but almost achieved 93%. There was no significant difference between the 2 methods at both criteria.

For OARs in all patient plans, the γ passing rates of CBCT plan doses obtained by HM and HD methods relative to those of

Table 2. The γ Passing Rates (Mean ± Std) of the 2 Methods at 3%/3mm Criterion, Along With the t and P Values of the Paired t-test Between the Passing Rates of the CBCT$_{HD}$ and CBCT$_{HM}$ Plan Doses.

	CBCT$_{HD}$ versus kVCT	CBCT$_{HM}$ versus kVCT	t	P
pGTV$_{nx}$	100.00 ± 0.01	99.91 ± 0.31	0.98	.348
pGTV$_{nd}$	99.16 ± 2.46	99.86 ± 0.29	−1.16	.270
PTV	98.25 ± 3.24	98.23 ± 3.99	0.01	.989
Parotid-L	100.00[a] ± 0	100.00[a] ± 0	-	-
Parotid-R	100.00[a] ± 0	100.00[a] ± 0	-	-
Oral cavity	100.00[a] ± 0	100.00[a] ± 0	-	-
L-E-T	99.99 ± 0.03	100.00 ± 0	−1.00	.356
Cord	100.00 ± 0	99.97 ± 0.11	1.00	.339
Body	99.92 ± 0.12	99.88 ± 0.23	0.58	.572

[a]t could not be calculated since the standard error of the difference is 0.

Table 3. The γ Passing Rates (Mean ± Std) of the 2 Methods at 2%/2 mm Criterion, Along With the t and P Values of the Paired t-test between the Passing Rates of the CBCT$_{HD}$ and CBCT$_{HM}$ Plan Doses.

	CBCT$_{HD}$ versus kVCT	CBCT$_{HM}$ versus kVCT	t	P
pGTV$_{nx}$	99.14 ± 1.50	99.14 ± 2.79	0.01	.994
pGTV$_{nd}$	96.52 ± 5.07	97.87 ± 3.95	−1.74	.107
PTV	91.65 ± 7.75	93.13 ± 7.66	−0.80	.440
Parotid-L	100.00[a] ± 0	100.00[a] ± 0	-	-
Parotid-R	99.99 ± 0.02	99.66 ± 0.86	1.34	.207
Oral cavity	100.00 ± 0.01	99.99 ± 0.02	1.30	.220
L-E-T	93.95 ± 8.66	95.21 ± 6.98	−0.71	.504
Cord	98.87 ± 2.58	99.15 ± 2.78	−0.28	.783
Body	99.26 ± 0.66	99.20 ± 0.93	0.29	.777

[a]t could not be calculated since the standard error of the difference is 0.

kVCT plan doses were higher than 99.99% at the 3%/3 mm criterion and reached higher than 93% at 2%/2 mm criterion. There were no significant dose differences between the 2 methods for all OARs.

Discussion

Comparing the dosimetric parameters of the targets and OARs, the mean deviation between the CBCT$_{HD}$ and CBCT$_{HM}$ plan doses was less than 1%. Taking kVCT plan doses as a reference, the γ passing rates for 2 CBCT plan doses at 2%/2 mm criterion were comparable. The tissues and organs of the head and neck contain dense substances such as air and bones; due to the relatively large density difference, it tends to produce streak artifacts and noise in the image. However, the HD curve used in the dose calculation was mainly based on fitting a specific density plug-in, which could not accurately reflect the tissues with different densities, resulting in a specific deviation. The accuracy of CBCT plan dose calculations using phantom calibration curves was no better than that using patient-specific or population-based CBCT curves.[21] Kong et al[29] suggested using DIR and HU override methods for volume delineation and dose computation: DIR could facilitate auto segmentation, while HU override could mainly be used to overcome the lower CBCT image quality.

This study used the Elastix registration tool to achieve rigid and deformable image registration in the in-house ART software. The efficacy of the registration tool was widely verified.[27] Also, the registration outcomes were visually evaluated for each data group in this experiment. Since it was difficult to match all images with any registration methods, image registration deviations caused unavoidable sources of error in the sequential dose calculation. Different deformable algorithms and parameters can lead to some deformation errors.[30] This study re-calculated the dose distribution using the HM and HD methods for each case in the same deformed CBCT images. By analyzing, we found that the registration accuracy affects the results of this work slightly.

Compared with the HM method, the HD method required more time to scan the phantom to make the curves of the CBCT image. In addition, dose calculation accuracy was more susceptible to image artifacts and individual differences in patient images, leading to unavoidable errors in the dose calculation process. Schröeder et al[31] investigated the effect on the dose calculation of a beam-shaping device used to reduce scattering. Consequently, the median γ passing rate was improved by 10.0% to 15.0%. In this study, all CBCT images were acquired with the Varian Clinac OBI system, with inferior image quality compared to newer systems by the same vendor, such as the TrueBeam and Halcyon kV CBCT systems. Moreover, more data, especially images with significant anatomical changes, might need to be added as a control group for validation in future studies. Artifact correction before CBCT calibration and DIR could improve the dosimetric accuracy by up to a 6.3% gamma passing rate.[32]

The dose calculation accuracy was acceptable using the HU modification method (HM) based on CBCT images. This way of dose calculation is more convenient for adaptive radiotherapy. HU modification using the histogram-matching algorithm for the artifacts caused by high-density substances and air in CBCT images can reduce the dose deviation.[33]

A deep convolutional neural or cycle-consistent generative adversarial network is also feasible to generate synthetic CT images based on CBCT images.[18,19,25,34,35] Most scatter artifacts of CBCT images could be removed[36] while the HU values were corrected to a certain extent. The promising results have been reported with different deep learning models (γ passing rates at 1%/1 mm improved from 88.2% to 96.3%[37] and from 94.5% to 99.0%[38]).

Conclusion

This study compared the dose calculation accuracy after correction of the CBCT using the HM and HD methods. The mean deviations between $CBCT_{HM}$ and kVCT plan doses were less than 1%, while the maximum value of deviations between $CBCT_{HD}$ and kVCT plan doses was 1.47% (L-E-T: $D_{2\%}$). Concerning dose distribution similarity, the γ passing rates of $CBCT_{HM}$-based plans relative to kVCT plan doses were higher than those of $CBCT_{HD}$ plan doses at the criterion of 2%/2 mm. In conclusion, the dose distribution deviations of $CBCT_{HM}$, $CBCT_{HD}$, and kVCT plan doses are not vastly different, proving that kVCT and CBCT hold a similar performance to be used for dose calculation. The calculated dose distribution all meet clinical application requirements. Based on the specific data set and implementation of this study, the CBCT images corrected by the HM method are more appropriate for RT planning utilization. These findings could guide us in selecting a more suitable method of CBCT correct method for adaptive radiotherapy of head and neck cancer patients.

Author contributions

Each author has participated sufficiently in the work to take public responsibility for appropriate portions of the content. SX designed the study and modified the paper. HG, XD, CX performed the study and analysis. BL developed software for adaptive radiation therapy. GZ was responsible for guiding the work. BQ and BC provide the patients' images. HG wrote the manuscript, and all other authors contributed to the manuscript and approved the final version.

Declaration of Conflicting Interests

The author(s) declared no potential conflicts of interest with respect to the research, authorship, and/or publication of this article.

Ethics Statement

This study was approved by the Ethics Committee of the Chinese PLA General Hospital (approved no. S2016-122-01).

Acknowledgment

ORCID iDs

Hanshun Gong https://orcid.org/0000-0001-8643-2549
Shouping Xu https://orcid.org/0000-0003-3189-9680

References

1. Diamantopoulos S, Platoni K, Patatoukas G, Karaiskos P, Kouloulias V, Efstathopoulos E. Treatment plan verification: a review on the comparison of dose distributions. *Phys Med*. 2019;67:107–115. doi: 10.1016/j.ejmp.2019.10.029.

2. Giacometti V, Hounsell AR, McGarry CK. A review of dose calculation approaches with cone beam CT in photon and proton therapy. *Phys Med*. 2020;76:243-276. doi: 10.1016/j.ejmp.2020.06.017.

3. Hvid CA, Elstrøm UV, Jensen K, Grau C. Cone-beam computed tomography (CBCT) for adaptive image guided head and neck radiation therapy. *Acta Oncol*. 2018;57(4):552-556. doi: 10.1080/0284186X.2017.1398414.

4. Posiewnik M, Piotrowski T. A review of cone-beam CT applications for adaptive radiotherapy of prostate cancer. *Phys Med*. 2019;59:13-21. doi: 10.1016/j.ejmp.2019.02.014.

5. Barker JLJr, Garden AS, Ang KK, et al. Quantification of volumetric and geometric changes occurring during fractionated radiotherapy for head-and-neck cancer using an integrated CT/linear accelerator system. *Int J Radiat Oncol Biol Phys*. 2004;59(4): 960-970. doi: 10.1016/j.ijrobp.2003.12.024.

6. Verellen D, De Ridder M, Tournel K, et al. An overview of volumetric imaging technologies and their quality assurance for IGRT. *Acta Oncol*. 2008;47(7):1271-1278. doi: 10.1080/02841860802244182.

7. Wang J, Hu W, Cai G, et al. Using corrected cone-beam CT image for accelerated partial breast irradiation treatment dose verification: the preliminary experience. *Radiat Oncol*. 2013;8:214. doi: 10.1186/1748-717X-8-214.

8. Chen S, Le Q, Mutaf Y, et al. Feasibility of CBCT-based dose with a patient-specific stepwise HU-to-density curve to determine time of replanning. *J Appl Clin Med Phys*. 2017;18(5):64-69. doi: 10.1002/acm2.12127.

9. Chai X, van Herk M, Betgen A, Hulshof M, Bel A. Automatic bladder segmentation on CBCT for multiple plan ART of bladder cancer using a patient-specific bladder model. *Phys Med Biol*. 2012;57(12):3945-3962. doi: 10.1088/0031-9155/57/12/3945.

10. Kim S, Yoo S, Yin FF, Samei E, Yoshizumi T. Kilovoltage cone-beam CT: comparative dose and image quality evaluations in partial and full-angle scan protocols. *Med Phys*. 2010;37(7):3648-3659. doi: 10.1118/1.3438478.

11. Rong Y, Smilowitz J, Tewatia D, Tomé WA, Paliwal B. Dose calculation on kV cone beam CT images: an investigation of the Hu-density conversion stability and dose accuracy using the site-specific calibration. *Med Dosim*. 2010;35(3):195-207. doi: 10.1016/j.meddos.2009.06.001.

12. Abe T, Tateoka K, Saito Y, et al. Method for converting cone-beam CT values into Hounsfield units for radiation treatment

planning. *Int J Med Phys Clin Eng & Radiat Oncol.* 2017;06(4):361-375. doi: 10.4236/ijmpcero.2017.64032.

13. Marchant TE, Joshi KD, Moore CJ. Accuracy of radiotherapy dose calculations based on cone-beam CT: comparison of deformable registration and image correction based methods. *Phys Med Biol.* 2018;63(6):065003. doi: 10.1088/1361-6560/aab0f0.

14. Giacometti V, King RB, Agnew CE, et al. An evaluation of techniques for dose calculation on cone beam computed tomography. *Br J Radiol.* 2019;92(1096):20180383. doi: 10.1259/bjr.20180383.

15. MacFarlane M, Wong D, Hoover DA, et al. Patient-specific calibration of cone-beam computed tomography data sets for radiotherapy dose calculations and treatment plan assessment. *J Appl Clin Med Phys.* 2018;19(2):249-257. doi: 10.1002/acm2.12293.

16. Veiga C, McClelland J, Moinuddin S, et al. Toward adaptive radiotherapy for head and neck patients: feasibility study on using CT-to-CBCT deformable registration for "dose of the day" calculations. *Med Phys.* 2014;41(3):031703. doi: 10.1118/1.4864240.

17. Veiga C, Alshaikhi J, Amos R, et al. Cone-beam computed tomography and deformable registration-based "dose of the day" calculations for adaptive proton therapy. *Int J Particle Ther.* 2015;2(2):404-414. doi:10.14338/IJPT-14-00024.1.

18. Hansen DC, Landry G, Kamp F, et al. Scatternet: a convolutional neural network for cone-beam CT intensity correction. *Med Phys.* 2018;45(11):4916-4926. doi: 10.1002/mp.13175. Epub 2018 Oct 8.

19. Landry G, Hansen D, Kamp F, et al. Comparing Unet training with three different datasets to correct CBCT images for prostate radiotherapy dose calculations. *Phys Med Biol.* 2019;64(3):035011. doi: 10.1088/1361-6560/aaf496.

20. Barateau A, Céleste M, Lafond C, et al. Calcul de dose de radiothérapie à partir de tomographies coniques : État de l'art [External beam radiotherapy cone beam-computed tomography-based dose calculation]. *Cancer Radiother.* 2018;22(1):85-100. French. doi: 10.1016/j.canrad.2017.07.050.

21. Richter A, Hu Q, Steglich D, et al. Investigation of the usability of conebeam CT data sets for dose calculation. *Radiat Oncol.* 2008;3:42. doi: 10.1186/1748-717X-3-42.

22. Dunlop A, McQuaid D, Nill S, et al. Comparison of CT number calibration techniques for CBCT-based dose calculation. *Strahlenther Onkol.* 2015;191(12):970-978. doi: 10.1007/s00066-015-0890-7.

23. Hu W, Ye J, Wang J, Ma X, Zhang Z. Use of kilovoltage X-ray volume imaging in patient dose calculation for head-and-neck and partial brain radiation therapy. *Radiat Oncol.* 2010;5:29. doi: 10.1186/1748-717X-5-29.

24. Zhang GS, Huang SM, Chen C, Xu SK, Zhang DD, Deng XW. Evaluating the therapeutic dose distribution of intensity-modulated radiation therapy for head and neck with cone-beam computed tomography image: a methodological study. *Biomed Res Int.* 2014;2014:326532. doi: 10.1155/2014/326532.

25. Kurz C, Maspero M, Savenije MHF, et al. CBCT Correction using a cycle-consistent generative adversarial network and unpaired training to enable photon and proton dose calculation. *Phys Med Biol.* 2019;64(22):225004. doi: 10.1088/1361-6560/ab4d8c.

26. Gong H, Xu S, Xu W, et al. Accuracy of dose calculation with CBCT images under different scanning conditions. *Chin J Med Instrum.* 2017;41(2):146-149. doi: 10.3969/j.issn.1671-7104.2017.02.019.

27. Klein S, Staring M, Murphy K, Viergever MA, Pluim JP. elastix: a toolbox for intensity-based medical image registration. *IEEE Trans Med Imaging.* 2010;29(1):196-205. doi: 10.1109/TMI.2009.2035616.

28. Onozato Y, Kadoya N, Fujita Y, et al. Evaluation of on-board kV cone beam computed tomography-based dose calculation with deformable image registration using Hounsfield unit modifications. *Int J Radiat Oncol Biol Phys.* 2014;89(2):416-423. doi: 10.1016/j.ijrobp.2014.02.007.

29. Kong VC, Marshall A, Chan HB. Cone beam computed tomography: the challenges and strategies in its application for dose accumulation. *J Med Imaging Radiat Sci.* 2016;47(1):92-97. doi: 10.1016/j.jmir.2015.09.012.

30. Song G, Han J, Zhao Y, Wang Z, Du H. A review on medical image registration as an optimization problem. *Curr Med Imaging Rev.* 2017;13(3):274-283. doi: 10.2174/1573405612666160920123955.

31. Schröder L, Stankovic U, Remeijer P, Sonke JJ. Evaluating the impact of cone-beam computed tomography scatter mitigation strategies on radiotherapy dose calculation accuracy. *Phys Imaging Radiat Oncol.* 2019;10:35-40. doi: 10.1016/j.phro.2019.04.001.

32. Thing RS, Bernchou U, Hansen O, Brink C. Accuracy of dose calculation based on artefact corrected cone beam CT images of lung cancer patients. *Phys Imaging Radiat Oncol.* 2017;1:6-11. doi:10.1016/j.phro.2016.11.001.

33. Arai K, Kadoya N, Kato T, et al. Feasibility of CBCT-based proton dose calculation using a histogram-matching algorithm in proton beam therapy. *Phys Med.* 2017;33:68-76. doi:10.1016/j.ejmp.2016.12.006.

34. Li Y, Zhu J, Liu Z, et al. A preliminary study of using a deep convolution neural network to generate synthesized CT images based on CBCT for adaptive radiotherapy of nasopharyngeal carcinoma. *Phys Med Biol.* 2019;64(14):145010. doi: 10.1088/1361-6560/ab2770.

35. Liang X, Dan N, Jiang SB. Generalizability issues with deep learning models in medicine and their potential solutions: illustrated with Cone-Beam Computed Tomography (CBCT) to Computed Tomography (CT) image conversion. *Mach Learn: Sci Technol.* 2021;2(1):015007(12pp). doi: 10.1088/2632-2153/abb214.

36. Zllner C, Rit S, Kurz C, Vilches-Freixas G, Landry G. Supplementary materials to "Decomposing a prior-CT-based cone-beam CT projection correction algorithm into scatter and beam hardening components". *Phys Imaging Radiat Oncol.* 2017;3:49-52. doi: 10.1016/j.phro.2017.09.002.

37. Liang X, Chen L, Nguyen D, et al. Generating synthesized computed tomography (CT) from cone-beam computed tomography (CBCT) using CycleGAN for adaptive radiation therapy. *Phys Med Biol.* 2019;64(12):125002. doi: 10.1088/1361-6560/ab22f9.

38. Wang T, Lei Y, Manohar N, et al. Dosimetric study on learning-based cone-beam CT correction in adaptive radiation therapy. *Med Dosim.* 2019;44(4):e71-e79. doi: 10.1016/j.meddos.2019.03.001.